Study of particle rotation effect in gas-solid flows using direct numerical simulation with a lattice Boltzmann method

Kyung C Kwon, Tuskegee University

L – S. Fan, Qiang Zhou, and Hui Yang, Ohio State University

Steven Seachman, DOE project manager

2013 UNIVERSITY COAL RESEARCH/HISTORICALLY BLACK COLLEGES AND UNIVERSITIES AND OTHER MINORITY INSTITUTIONS CONTRACTORS REVIEW MEETING, 06/11 – 06/13/2013

Presentation Outline

- Background
- Objectives
- Research Setup
- Upgrade of the Existing Code
- Capabilities of the Upgraded Code
- Drag Force and Lift Force
- Validation of the new IB-LBM code

    1. Simple cubic lattice of fixed spheres
    2. Drag force for ordered arrays
    3. Unsteady flows with very low Reynolds numbers
    4. Drag force for frozen ordered arrays
    5. Normalized drag force and lift force

- Practical applicability of lift force
- Summary
- Further work

Background

- Gas-solid multiphase flows are prevalent in many fossil fuel processes such as gasification and combustion.

- Advanced computational technique known as the computational fluid dynamics (CFD) has been recognized as an emerging tool that is able to reduce the computing time and cost in the design and scale-up of the multiphase reactors involved in those processes, and has been applied in typical equipment such as fluidized bed gasifiers and chemical looping combustion reactors.

- The capability of the CFD in correctly predicting multiphase flow dynamics relies heavily on accuracy of sub-models that account for particle-fluid interactions and particle-particle interactions.

- The overall objective of our proposed research is to improve fundamental understanding of such interactions, and to formulate a new drag model incorporated into particle rotation effects that can be applied to reactor scale simulations

Schematic of the KBR Transport Gasifier (TRIG)

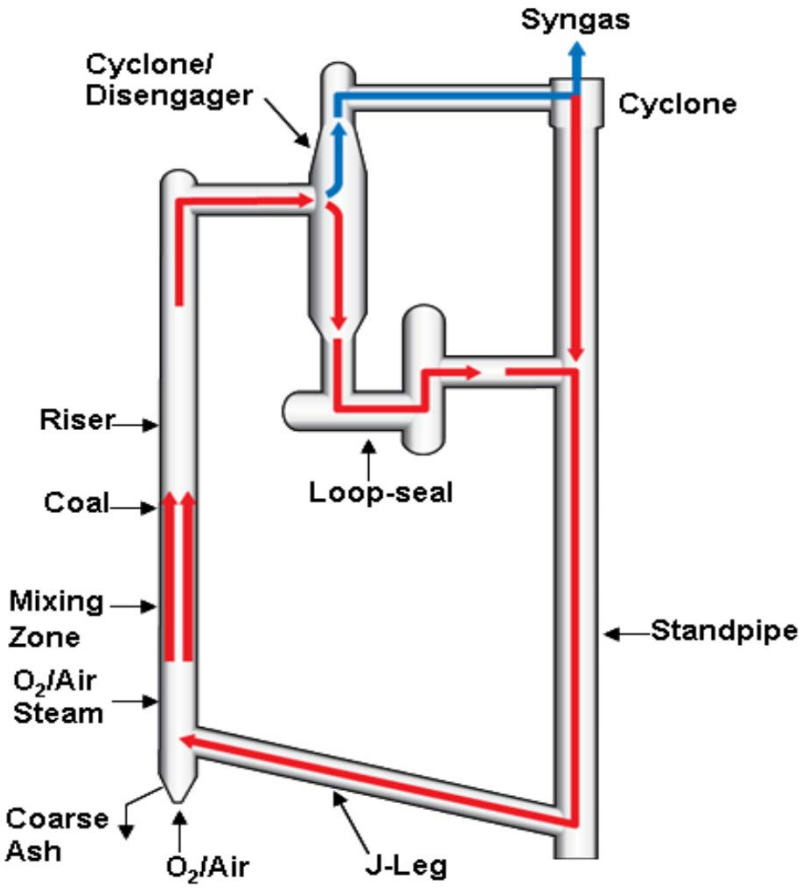

Coal Gas Cleanup

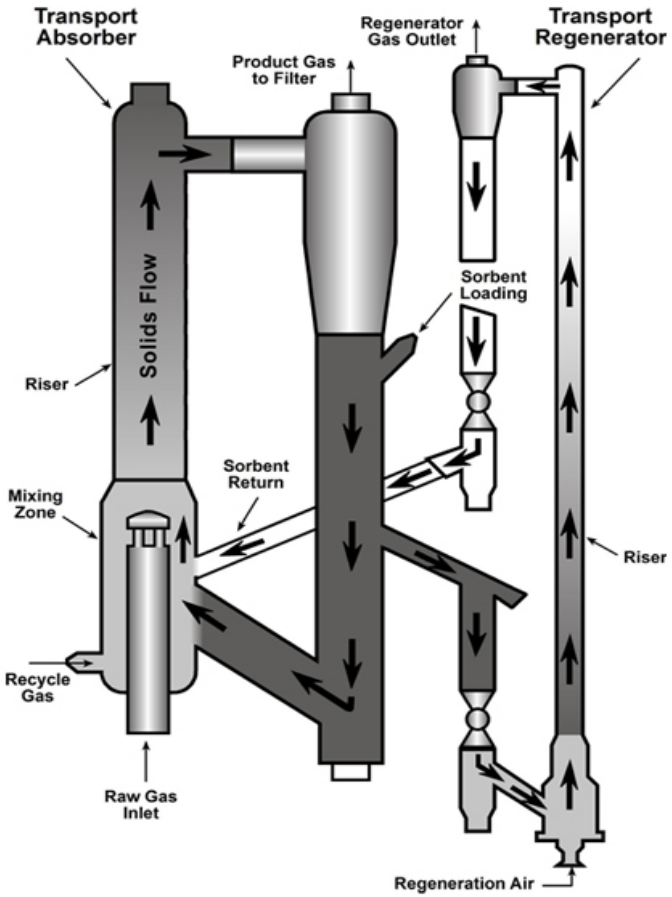

Catalytic Cracker

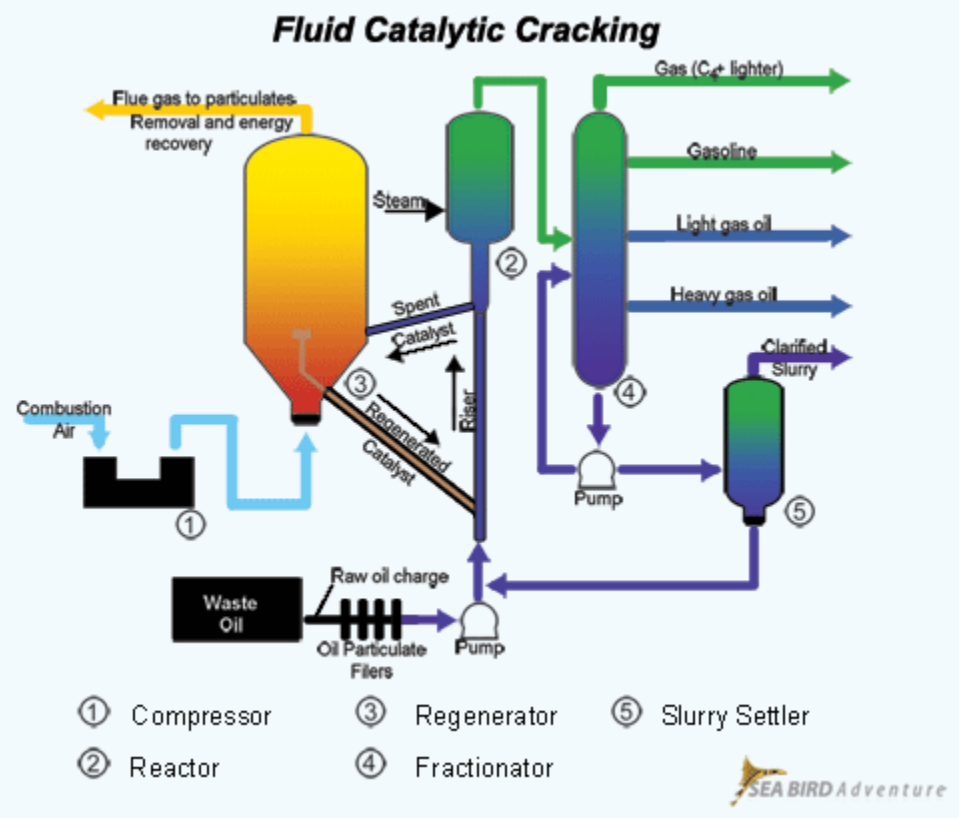

Objectives

The emphasis of our simulation work is to address effects of particle rotation in gas-solid flows with the following specific aims:

- direct impact of particle rotation on the average particle-fluid drag force of a particle suspension at various particle and rotational Reynolds numbers.

- indirect impact of particle rotation on the drag force through the change in the particle concentration distribution, or the microstructure of a flow.

- role of particle rotation in energy dissipation of the particle-fluid system.

Research Setup

Hardware

Workstation
Supercomputer

Software

Linux Operating system
Gfortran compiler
MFIX code from DOE/NETL

Human Beings

Developing computer software codes with hardware and software to achieve our objectives

References

Literature data to verify our simulation

Upgrade of the Existing Code

Modification of the existing code for direct numerical simulations of gas-solid flow has been completed by

- adopting the multi-direct forcing method in the improved immersed boundary method (IBM),
- retracting slightly the Lagrangian grid from the surface of a particle towards the interior of the particle with a fraction of the Eulerian grid spacing,
- developing an over-relaxation technique in the procedure of multi-direct forcing method, and
- implementing the classical fourth order Runge-Kutta scheme in the coupled fluid-particle interaction.

Capabilities of the Upgraded Code

The second-order accuracy for simulations of translational and rotational motions of particles can be achieved through the new improved code and hence shortening computing times.

Drag Force and Lift Force

- The lift force is defined as the force that is exerted on the surface of a spherical particle perpendicular to the direction of a fluid flow, whereas the drag force is defined as the force that is exerted on the surface of a spherical particle in the opposite direction of a fluid flow.
- The rotational Reynolds number is used to characterize the rotational movement of spheres.

$$Rer = \omega D^2/\nu$$

ω: angular velocity of a spherical particle
D: diameter of a spherical particle
ν: kinematic viscosity of a fluid

Simple cubic lattice of fixed spheres

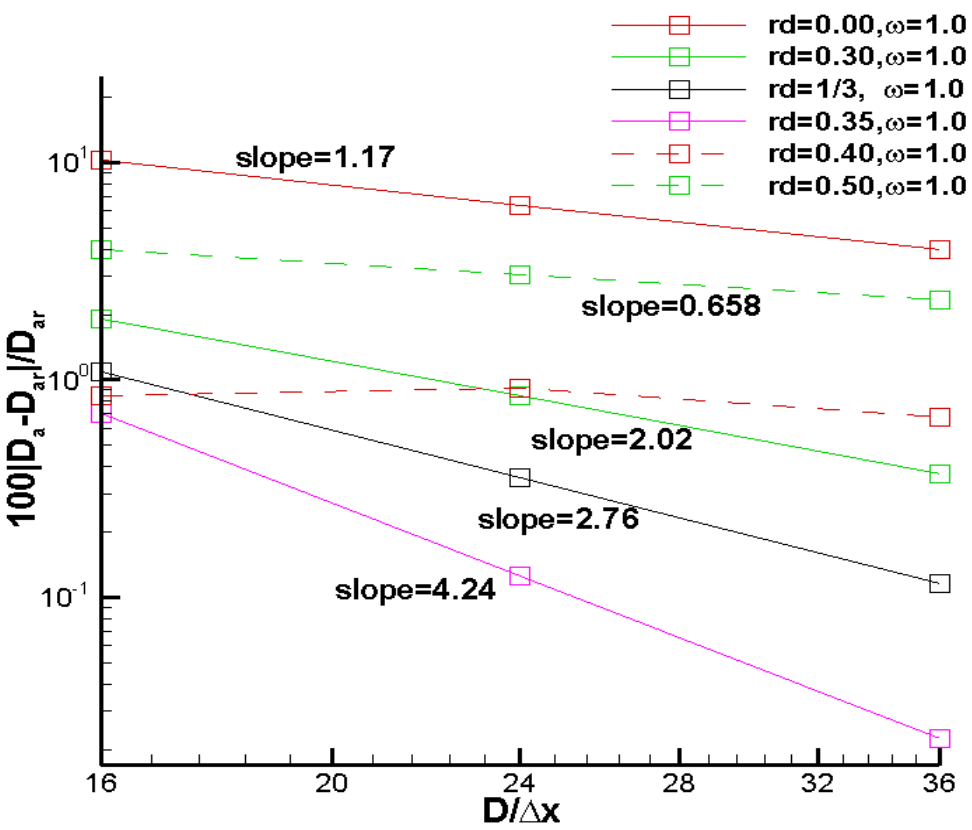

Figure 2, Percentage error in Darcy number D_a as function of the grid resolution at various retraction distances. The error is relative to the value of the Darcy number D_{ar} obtained from Richardson extrapolation [4] using the data points of $D/\Delta x$= 16, 24 and 36.

[1]. Breugem W. P.. A second-order accurate immersed boundary method for fully resolved simulations of particle-laden flows. Journal of Computational Physics. (2012) 231 4469-4498.12

[4]. Ferziger J.H., Peric M.. Computational Methods for Fluid Dynamics, Springer-Verlag,Berlin, 2002.

- Laminar flow through a simple cubic lattice of fixed spheres [1] was simulated to obtain Darcy's number.
- Percentage errors in Darcy number D_a are plotted as function of the grid resolution at various retraction distances to obtain convergence accuracy [1].
- The combination of LBM and the classical fourth-order Runge-Kutta scheme for the convergence of Darcy's number improved our simulation to second-order accuracy.
- The accuracy of numerical simulations becomes more than second order over the r_d range between 0.30 and 0.35

$$Da = \frac{\mu_f U_b}{(-dp_e/dx)D^2}.$$

D: diameter of spheres D_r: retraction distance
D_a: Darcy's number $r_d = D_r / \Delta x$
Δx: Eulerian grid spacing
r_d : dimensionless retraction distance
μ_f: viscosity of a fluid
$\boldsymbol{U}_b$: bulk velocity of a fluid
dPe/dx: pressure gradient

Unsteady flows through spheres in simple cubic arrays at very low particle Reynolds number

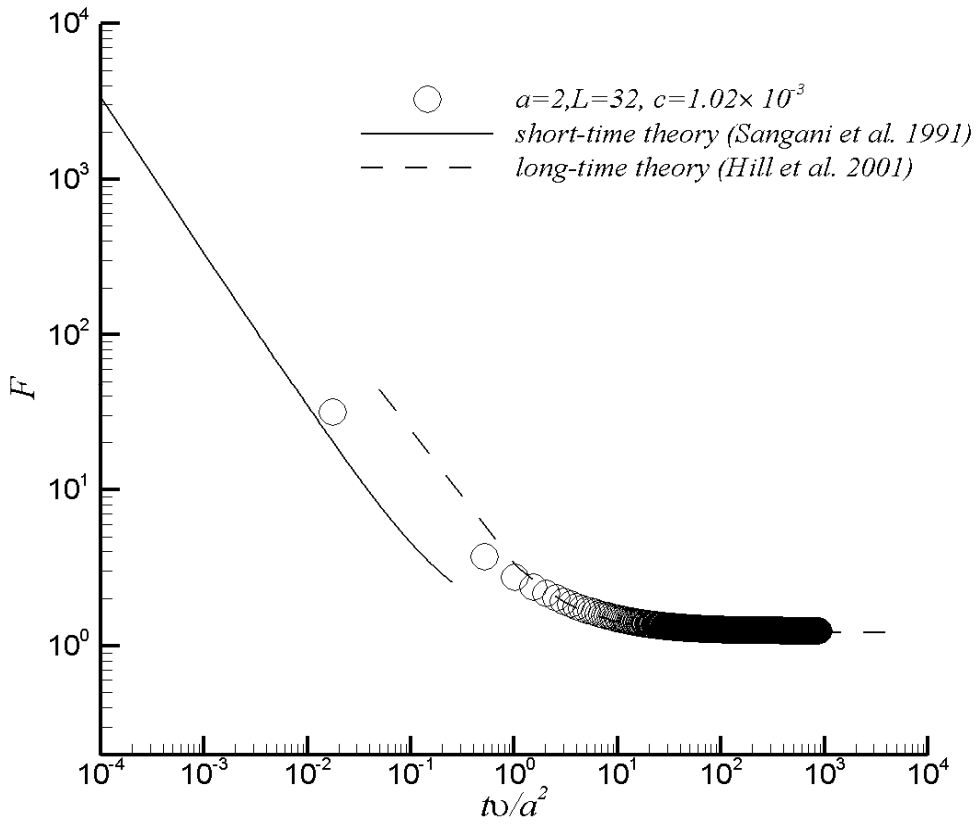

Figure 4. The time series of the non-dimensional drag force on the spheres in simple cubic arrays when the fluid is accelerated from rest by a constant average pressure gradient toward a steady Stokes flow.

a denotes the radius of the sphere, *L* denotes the dimension of the computational domain, and *c* is the solid volume fraction. ν: kinematic viscosity of a fluid. τ : characteristic relaxation time of a fluid flow

- Evolution of average velocity and drag force on spheres in simple cubic arrays are examined when the fluid is accelerated from rest toward a steady Stokes flow by a constant body force.
- Results of our simulation of the unsteady non-dimensional drag force on the spheres in simple cubic arrays agree well with the theoretical predictions both at the short times [9] and at the long times [8].
- This demonstrates that the improved IB-LBM code can simulate the unsteady fluid-solid flow accurately.

[8] Hill R.J., Koch D.L., Ladd A.J.C., The first effects of fluid inertia on flows in ordered and random arrays of spheres. J. Fluid Mech., (2001) 448: 213-241.

[9] Sangani, A. S., Zhang, D. Z. & Prosperetti, A. The added mass, Basset, and viscous drag coefficients in non-dilute bubbly liquids undergoing small-amplitude oscillatory motion. Phys. Fluids A (1991)3, 2955-2970.

Normalized Stokes-flow drag force on non-rotational fixed spheres as a function of $1/r_h^2$

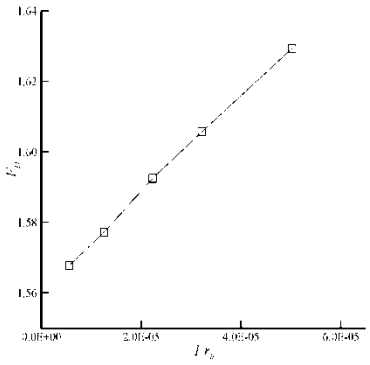

(a) *C = 0.01*

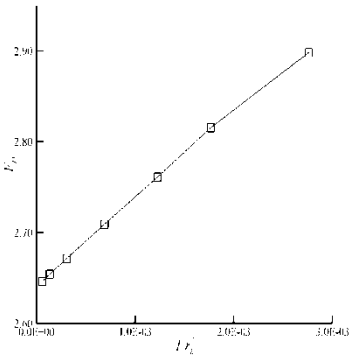

(b) *C = 0.06545*

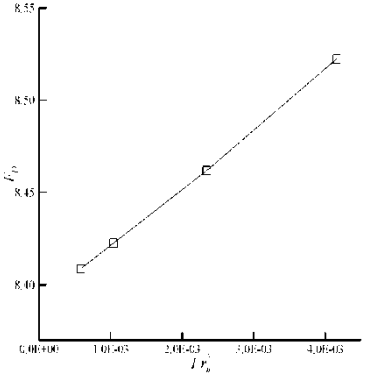

(c) *C = 0.3*

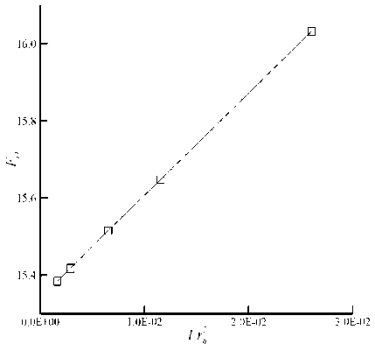

(d) *C = 0.45*

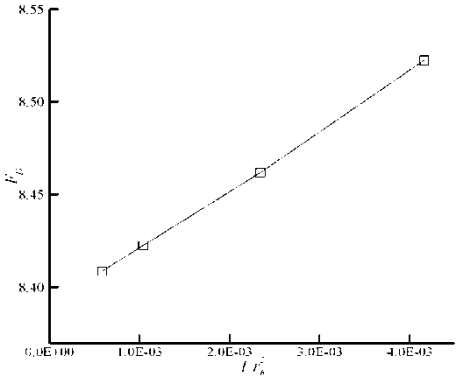

(e) *C = 0.5*

Figure 1. Normalized Stokes-flow drag force on the non-rotational spheres as a function of . The simulated results forms a straight line as approach zero, indicating the simulations have a second-order convergence rate. The solid volume fractions for (a), (b), (c), (d) and (e) are 0.01, 0.06545, 0.3, 0.45 and 0.5, respectively.

$$r_h = D(1-c) / 6c$$

r_h: hydraulic radius, D: diameter of particles,
c : solid volume fraction,

- Van der Hoef et al [2] pointed out that simulated drag forces are converging with the second-order accuracy when plots of drag force against $1/r_h^2$ form a straight line.
- The simulated results form a straight line as $1/r_h^2$ approach zero, indicating the simulations do have a second-order convergence rate [2].

[2] Van der Hoef M. A., Beetstra R., Kuipers J. A. M., Lattice-Boltzmann simulations of low-Reynolds-number flow past mono- and bidisperse arrays of spheres: results for the permeability and drag force. J. Fluid Mech. (2005) vol. 528, pp. 233-254

Normalized Stokes-flow drag force on non-rotational fixed spheres in simple cubic arrays at various solid volume fractions

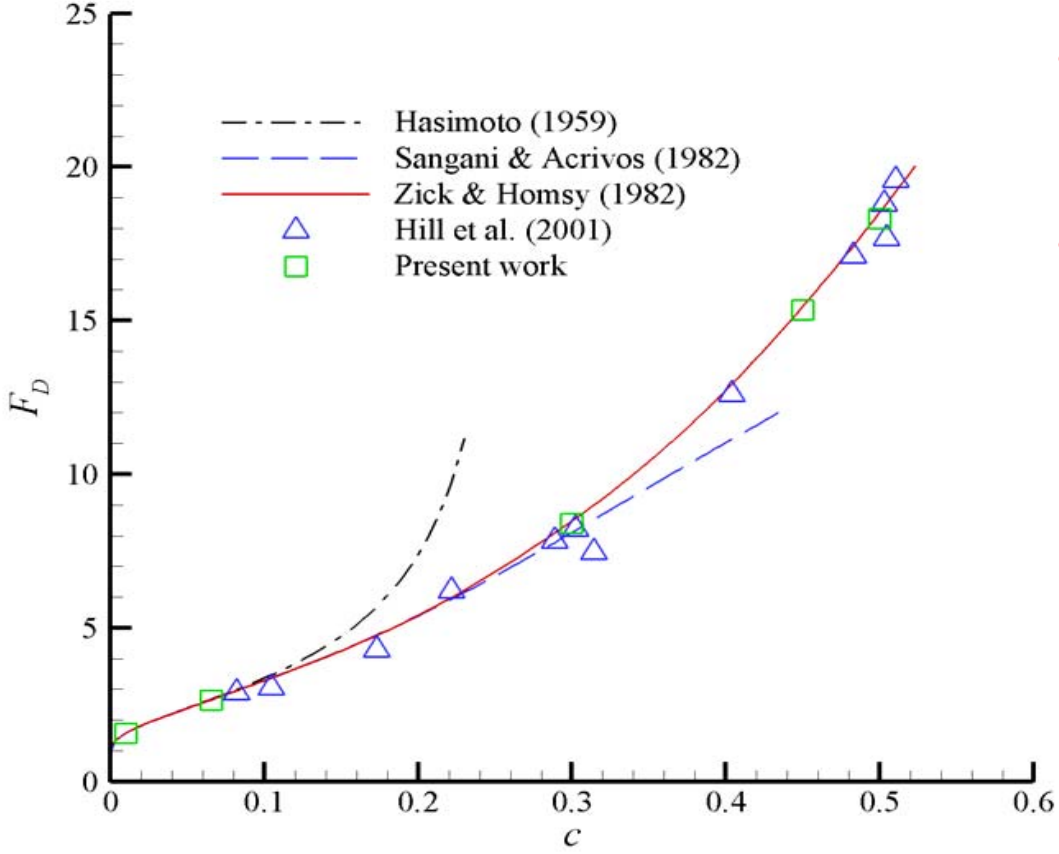

Figure 2. The normalized Stokes-flow drag force on the non-rotational spheres in simple cubic arrays as a function of the solid volume fraction. The simulation result of Hill et al. [7] and the results from the theories of Hasimoto [4], Sangani & Acrivos [5] and Zick & Homsy [6] are also shown

- Our results are in excellent agreement with the theory of Zick & Homsy [6].
- The comparison of the data in Figure 2 demonstrates that the present upgraded IB-LBM code can predict the drag force accurately.

[4] Hasimoto, H. On the periodic fundamental solution of the Stokes equations and their application to viscous flow past a cubic array of spheres. J. Fluid Mech. (1959) 5, 317-328.

[5] Sangani, A. S. & Acrivos, A. Slow flow through a periodic array of spheres. Intl J. Multiphase Flow (1982) 8, 343-360

[6] Zick, A. A. & Homsy, G. M. 1982 Stokes flow through periodic arrays of spheres. J. Fluid Mech. 115, 13-26.

[7] Hill, R. J., Koch, D. L. & Ladd, A. J. C. The first effects of fluid inertia on flows in ordered and random arrays of spheres. J. Fluid Mech. (2001) 448, 243-278

Normalized Stokes-flow lift force as a function of $1/r_h^2$ at c = 0.06545 or 0.5 and Re_r=0.1 or 100

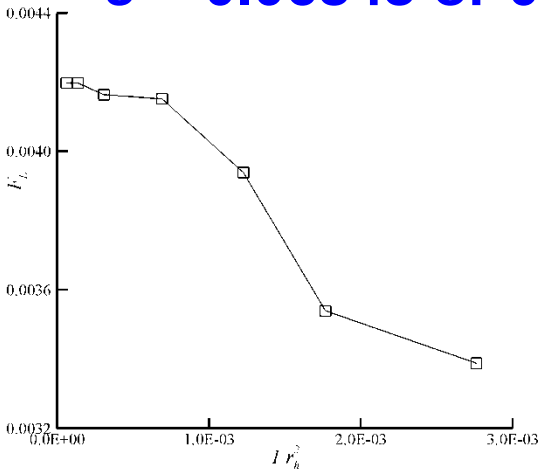

(a) *C = 0.06545, Rev = 0.1*

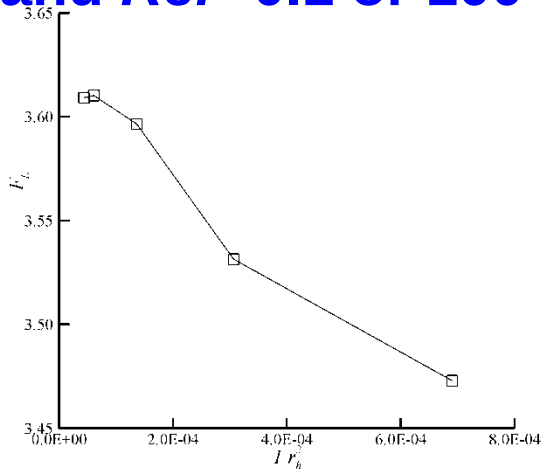

(b) *C = 0.06545, Rev = 100*

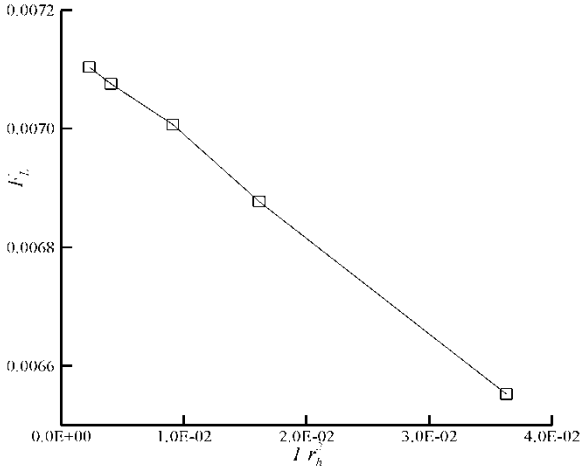

(c) *C = 0.5, Rev = 0.1*

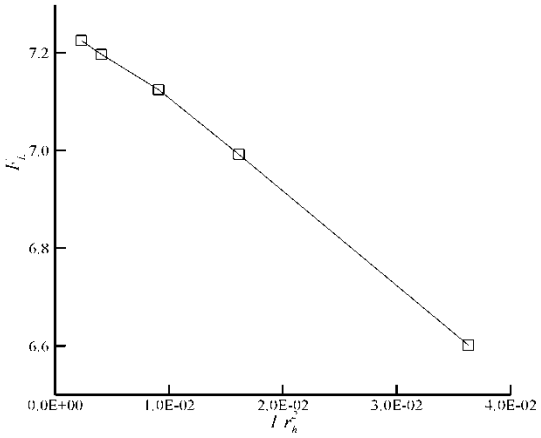

(d) *C = 0.5, Rev = 100*

Figure 3, Normalized Stokes-flow lift force as a function of $1/r_h^2$ at the solid volume fractions of 0.06545 and 0.5 and the rotation Reynolds numbers of 0.1 and 100.

- The lift force is also normalized by the Stokes drag force of infinite dilution for the convenience of the comparison.
- The lift force does not follow a second-order convergence at the low solid volume fraction (e.g., 0.06545). In this situation, the mesh is refined until the two finest meshes give indistinguishable results. The value on the finest mesh will be used for later analysis.
- The lift force forms a straight line as the drag force does at the high solid volume fraction, e.g., c=0.5, indicating that the convergence rate is second order. In this case, the final value of the lift force will be calculated by the Richardson extrapolation.

Normalized drag force and lift force as a function of *rotational Reynolds numbers* at *various solid volume concentrations*

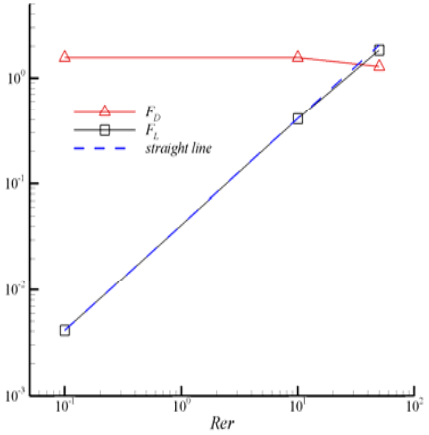

(a) *C = 0.01*

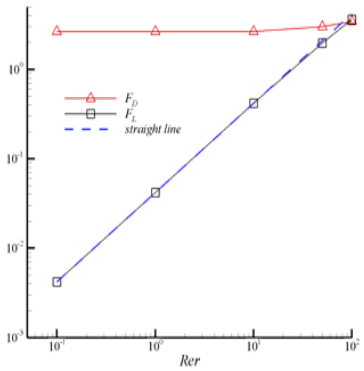

(b) *C = 0.06545*

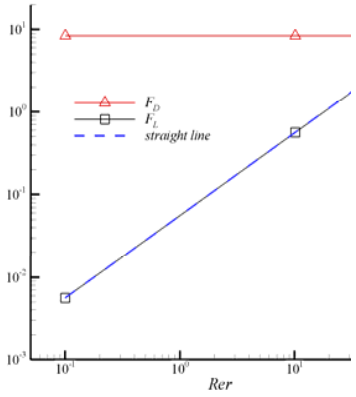

(c) *C = 0.3*

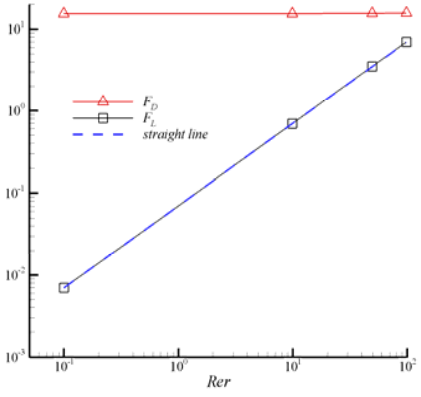

(d) *C = 0.45*

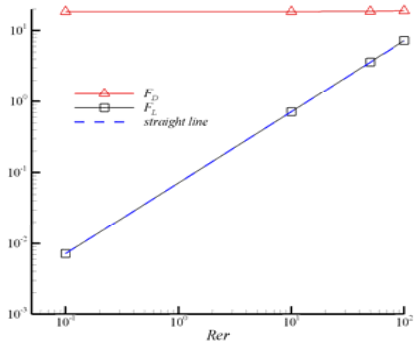

(e) *C = 0.5*

Figure 4. The normalized Stokes-flow drag force and lift force are shown as a function of rotational Reynolds numbers *Rer* . The plots of lift forces as a function of Reynolds numbers in the Figure (a) through (e) show a straight line FL(c, Rer) = , passing through the point of $F_L(c, Rer{=}0.1)$. *C* = solid volume fraction. The solid volume fractions for the figures (a), (b), (c), (d) and (e) are 0.01, 0.06545, 0.3, 0.45 and 0.5, respectively.

- The drag forces only have noticeable deviations from the horizontal line as the particle Reynolds number increases at the low solid volume fractions of 0.01 and 0.06545.
- The drag force doesn't change very much as the rotational Reynolds number varies at very low rotational Reynolds numbers.
- The lift force is nearly perfectly proportional to the rotational Reynolds number. All the simulated lift forces satisfy the formula described in Equation 3.

$$F_L(c, Rer) = F_L(c, Rer)|_{Rer=0.1} Rer/0.1 \qquad (3)$$

- Equation 3 also indicates that the lift force can be very significant at high rotational Reynolds numbers.
- Figure (a) shows that the lift force is around 43% of the drag force at the solid volume fraction of 0.01 and the rotational Reynolds number of 50.
- Figure (e) shows that the lift force is around 39% of the drag force at the solid volume fraction of 0.5 and the rotational Reynolds number of 100. The lift force would be as strong as the drag force at the solid volume fraction of 0.5 and the rotational Reynolds number of around 250.

Practical applicability of lift force to a coal gasifier

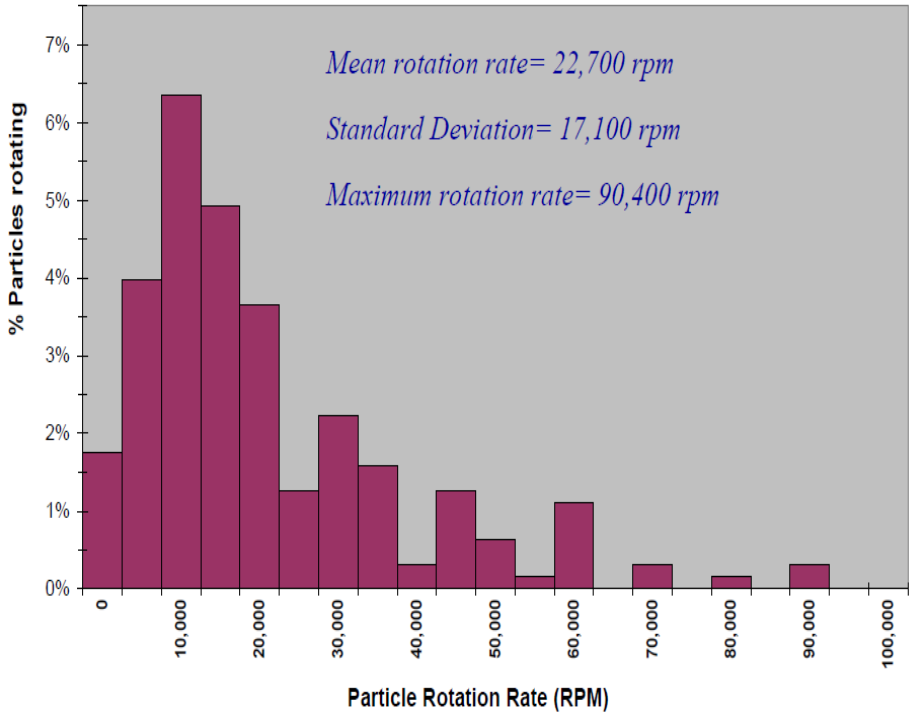

- Recently, high speed imaging has shown that about 20% of particles are rotating at high speeds in a riser flow field. Based on the measurements conducted by Shaffer et al. [9], the average rotation rate of particles in the riser flow is around 22,700 rpm and the maximum rotation rate can reach as high as 90,400 rpm.
- Considering that the diameter of particles they used is around 750 microns, the corresponding rotational Reynolds numbers of the mean and maximum rotations rates are 130 and 520, respectively.
- Therefore, our simulations of lift forces at the rotational Reynolds number up to 100 are not outside of the practical range and thus are helpful for researchers to understand that the lift force is not negligible in simulating fluid-solid flows. In previous simulations, effects of the particle rotation on lift forces are not considered

[9] Shaffer, F., Shadle, L., & Breault R. High Speed Particle Imaging: Visualization and Measurement of High Concentration Particle Flow. NETL multiphase Flow Workshop, Morgantown, WV, April 22-23, 2009.

Summary

- The existing IB-LBM code is modified and upgraded to the second-order convergence accuracy from the first-order one.
- The lift force generated by the rotation movement of solid particles is insignificant at rotational Reynolds numbers below 0.1. However, it can be larger than the drag force especially at low solid volume fractions and high rotational Reynolds numbers.
- The lift force caused by the rotation movement of a particle is directly proportional to rotational Reynolds numbers and the drag force is barely affected by rotational Reynolds numbers.
- Our simulations demonstrated that the lift force caused by the particle rotation can be very significant compared to the drag force and must be considered in further study on two-fluid simulations.

Further Work

- Simulations of solid particles in practical random arrays will be performed at various particle Reynolds numbers and rotational Reynolds numbers to compute the average drag and lift forces exerted on spheres over the entire range of the solid volume fraction up to the close-packed limits.

- The drag law and the lift law for solid particles in random arrays will be obtained and tested in two-phase fluid simulations.

Future Work

- Micro-structures of particles
- Translational and rotational fluctuations
- Install new drag models into MFIX
- Perform simulations of selected experimental gas-solid risers
- Compare new drag models with existing drag models